Plain bearing stresses due to forming and oil film pressure

A. Burke-Veliz[1], D. Wang[2], N. Wahdy[2], P.A.S. Reed[1], D. Merritt[2], S. Syngellakis[1].

[1]University of Southampton, School of Engineering Sciences, Southampton SO17 1BJ, UK.

[2]MAHLE Engine Systems UK Ltd, 2 Central park Drive, Rugby CV23 0WE, U.K.

allan.burke@itesm.mx

Abstract. This paper describes a methodology for assessing critical stress ranges arising in automotive plain bearings during engine operations. An industry-produced and run simulation program provides information on oil film pressure and overall bearing deformation during accelerated performance tests. This code performs an elasto-hydrodynamic lubrication analysis accounting for the compliance of the housing and journal. Finite element analyses of a multi-layer bearing are performed to assess the conditions responsible for possible fatigue damage over the bearing lining. The residual stresses arising from the forming and fitting process are first assessed. The stress analyses over the engine cycle show the intensity and distribution of cyclic tensile and compressive stresses in the bearing. The location of maximum stress range is found to be consistent with the damage observed in accelerated fatigue tests. Critical zones are identified in the lining for possible fatigue crack initiation and growth studies.

1. Introduction

The introduction of new materials and design processes in the automotive industry, driven by the quest for improved power efficiency, has resulted in smaller, more lightweight and durable components, which however operate under more demanding service conditions. The design of plain bearings is one case in point, because of their importance to the powertrain system and their strategic position within the engine. The bearing design process is complex and involves assessment of manufacture, assembly and service conditions. The study of the latter is especially interesting and challenging since it is currently based on elasto-hydrodynamic lubrication (EHL) analyses whereby the hydrodynamic oil film pressure is coupled with the elastic deformation of the housing and the journal. The predicted film pressure, shown schematically in Figure 1, is characterized by steep gradients, which may lead to damage over the bearing surface arising from fatigue, wear, cavitation erosion and fretting among others.

The study of fatigue damage in plain bearings has mainly involved semi-empirical approaches to the assessment of the total service life. Thus, the number of cycles to failure has been linked to the specific load, that is, the load applied through the connecting rod divided by the projected bearing area. Simplified two-dimensional [1-3] and, to a lesser extent, three-dimensional [4] finite element analyses of bearings under hydrodynamic film pressure have attempted to link the likely position of fatigue crack initiation and growth to the maximum tensile tangential stress developing in the bearing lining.

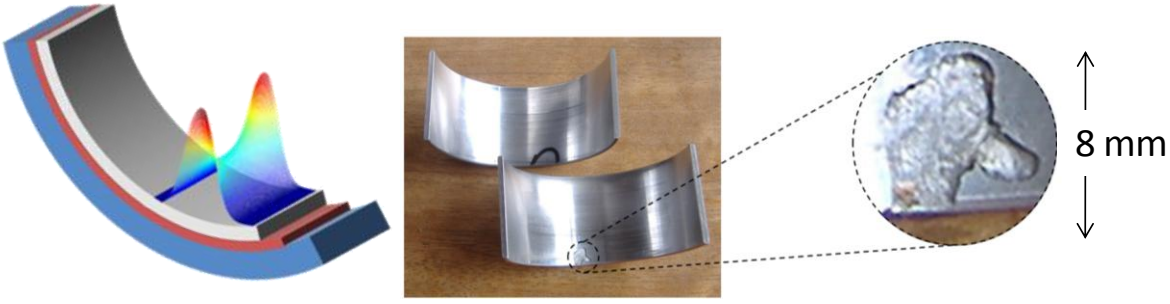

Figure 1. Tri-layer bearing with representative hydrodynamic film pressure profile (left) and fatigue damage in the lining (right).

The elastic flat strip models by Martin et al [1] and bearing shell by McCallion and Lofti [2] showed a good correlation between the fatigue crack origins in test specimens and their assessments of the maximum tangential stress. In the early 1990s, Bahai and Xu [3] predicted the stresses due to the oil film pressure through an axisymetric elasto-plastic finite element bearing shell model; they concluded that tensile deviatoric tangential stresses are present at the observed crack initiation site during the whole engine cycle while their hydrostatic counterpart dominates the overall stress state in a compressive environment. Hacifazlioglu and Karadeniz [4] studied the effects of the housing rigidity and bearing surface discontinuities on tangential tensile stresses in a three-dimensional flat strip model. Perez et al [5] used an elastic bearing shell model to assess the effects of housing rigidity as well as backing stiffness and lining thickness on tangential stresses. The influence of manufacturing and assembly processes on bearing performance was not accounted for in these studies. The incorporation of the forming process and interference fit, in particular, into an integrated analysis procedure is therefore an area where further work is necessary.

Appropriate design methodologies play a major role in the life cycle of modern products; it is also essential to produce high quality components in the shortest possible time. Therefore, tailored design strategies have been developed for automotive plain bearings in order to satisfy customer needs. They are based on analysing three major contributors to stress development: fitting of the bearing in its housing, internal forces in the engine and hydrodynamic oil film pressure. Standard, efficient design procedures in MAHLE Engine Systems rely on exact solutions and two-dimensional EHL analyses to evaluate the bearing interference fit stresses and hydrodynamic film pressure on the bearing surface, respectively.

Advanced three dimensional analyses employed by MAHLE include more sophisticated techniques that take into account the bearing stiffness, wear and surface profile among other factors. Initially, the assembly process is simulated leading to the resulting bearing deformation; this is achieved through non-linear FE contact analysis, based on the general-purpose package ABAQUS [3]. Thus, the bearing shape and clearances between the bearing and housing surfaces are estimated. Using the finite difference in-house code SABRE-EHL [6, 7], it is possible to estimate the hydro-dynamic oil film pressure and housing deformation during a complete engine cycle. At the same time, different indicators related to strength, wear, cavitation erosion and fretting are generated to assess the propensity for damage.

In this work, this design methodology was taken one step further using oil film pressure and housing deformation estimates from SABRE-EHL to generate detailed information about the stresses arising in the bearing. The analysis of manufacturing and service conditions was combined to provide a global view of the possible failure mechanisms in bearings. Based on simplifying assumptions, the forming process was simulated for an initial evaluation of a realistic distribution of residual stresses to be incorporated into the stress analysis under service conditions. The latter analysis is expected to lead to a better understanding of the influence of complex and changing film pressure and concomitant housing deformation under EHL conditions on bearing performance. Thus, it will be possible to assess

the importance of particular geometric and material parameters and correlate them with experimental observation of lining detachment, a condition that is particularly harmful to bearing performance.

2. Methodology

2.1. Component modelling

SABRE-EHL carries out a coupled analysis to compute the oil film pressure throughout an engine cycle. This involves a heat balance analysis to determine the oil viscosity and material expansion leading to estimates of the clearances between bearing and journal. Extended SABRE-EHL analyses may include the input of oil feed and journal profile, account for grooves and elliptical shapes as well as solid-to-solid contact with flexible components. The latter requires the input of the elastic compliances of both the housing-bearing assembly and the journal [7]. Hence, the housing deformations are estimated during the process and, together with the oil film pressure, are later transferred to the FE stress analysis of just the bearing to assess its behaviour under service conditions.

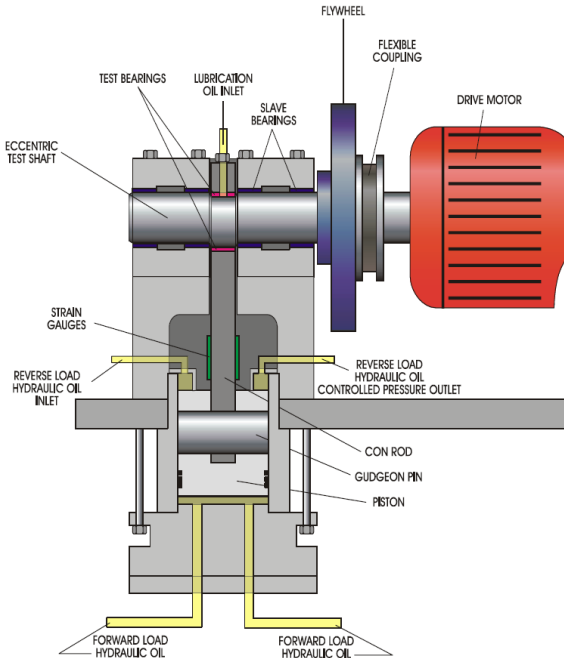

Figure 2. Sapphire test rig

The stresses and deformations experienced by the bearing are clearly dependent on the engine design and, in particular, on the specific load and housing distortion generated during the combustion cycle. Light and flexible housings promote large deflections in the bearing and may lead to premature bearing damage. The assessment of bearing architectures within MAHLE Engine Systems is carried out through an accelerated performance testing procedure using a standardised housing with enhanced stiffness. Such a test is carried out on a rig, shown schematically in Figure 2, designated as Sapphire [6]. It consists of an eccentric shaft that forces a piston to travel in the vertical direction through a connecting rod. At the same time, the rig applies some resistance to the movement of the piston due to the oil present in the chamber of a hydraulic ram. This oil is forced into another chamber and its flow is regulated by valves to obtain the desired resistance of travel or specific load applied to the bearing. The precise measurement of the load applied to the bearing is carried out through strain gauges positioned at the connecting rod. A great amount of experimental fatigue data are generated under such conditions; this makes the Sapphire rig output an ideal candidate for comparison with the results of numerical simulations. For this reason, SABRE-EHL analyses have been extensively applied to various Sapphire rig testing conditions and the output entered into subsequent stress analyses.

2.2. Bearing forming simulation

For this particular study, a tri-layer bearing architecture was analysed using a three dimensional FE bearing shell model built on ANSYS 11.0, a general purpose finite element package [8]. The analysis was based on a multi-linear elasto-plastic strain hardening and large deformation theory.

The first part of the numerical work dealt with the forming process generating a concave shell from a flat strip; previous manufacturing operations were not simulated given that thermal treatment relieves residual stresses developing prior to the forming operation. The simulation of the forming process and the estimation of residual stresses were carried out through the modelling of an initially

flat, multi-layered strip placed between a punch and a die of identical semi-circular profile. Only half of the bearing was modelled by assuming symmetry with respect to the mid-plane across its width. This is consistent with the format of the output generated by the component model. The analysed tri-layer architecture consisted of a backing layer, an interlayer and lining layer whose properties and thicknesses are listed in Table 1. The length of the strip was set such that it would form a half bearing shell of 26.4 mm outer radius and a width of 29 mm.

Table 1. Material properties of layers

Layer	Material description	Thickness (mm)	Young's Modulus (GPa)	Poisson Ratio	Yield stress (MPa)	Ultimate stress (MPa)	Strain hardening exponent
Lining	Aluminium alloy	0.38	70	0.33	53	166	0.238
Inter-layer	Pure aluminium	0.04	67	0.33	37	78	0.19
Backing	Low-carbon steel alloy	1.8	198	0.3	459	512	0.058

Apart from the material non-linearity arising from elasto-plastic material behaviour, the analysis also involves geometric non linearity due to contact between the forming tools and the strip. Friction was included in contact modelling with a coefficient of friction of 0.1 [9]. For the sake of computational efficiency, both die and punch were modelled as rigid due to their stiffness being much higher than that of the flat strip. The mesh of the flat strip was built according to that used in SABRE-EHL to simplify the application of boundary conditions in later analysis and transfer of residual stress data, which are associated with the elements and their internal integration points.

Initial simulations involving the tri-layered architecture exhibited a non-convergent behaviour, which probably arose from the considerably lower stiffness and strength of the interlayer compared to those of the backing and the lining. This problem also arose in the initial attempts at stress analysis of the bearing under service conditions and can be addressed by refining the mesh and increasing the solution steps. Such measures however lead to excessive computational cost. For this reason, the interlayer was initially considered as part of the lining leaving the assessment of its structural influence on the overall stiffness of the component to a later stage.

The forming simulation was carried out in four stages. During the initial phase when the punch comes into contact with the flat strip, the latter deflected by only 2.5% of the total forming depth requiring a large number of iterations to reach a numerically stable stage. The main deformation stage was more stable but it required a large number of solution steps to complete the travel of the punch to the bottom of the die. During the load release stage, some contact between the punch and the flat strip is maintained because of the spring back force. Finally, an additional upward displacement was imposed on the bearing to overcome the frictional force keeping it attached to the die.

2.3. Stress analysis under service conditions

The residual stresses generated by the bearing forming simulation were taken into account at this stage of the analysis by transferring them into the bearing FE model. As already mentioned, the mesh used in this model was consistent with the mesh of the component model as well as that of the forming analysis to simplify the post-processing operations. An additional step was introduced at the beginning of the analysis to account for the fitting deformations that occur during assembly. Relevant modelling performed at MAHLE predicted that fitting causes a housing radial displacement of around 0.028 mm; this was applied to the outer backing surface.

Pressures and housing deformations obtained from SABRE-EHL simulating Sapphire rig operation were applied, respectively, to the lining surface and the outer backing surface of the model. The performed stress analysis corresponded to an experimental set up at 3000 rpm, a specific load of 97 MPa and oil feed temperature of 140º. The respective film pressure and housing deformation are shown in Figure 3 over half of the model; a peak pressure of around 200 MPa occurs when the crank angle is 180° with the 0º position at the centre of the top bearing shell (further from the connecting rod). A grid of 2002 points was used at intervals of 2 degrees over the engine cycle. The manipulation process of this data for the purpose of stress analysis was carried out in MATLAB 7.3, where only 36 load steps at intervals of 10 degrees were applied due to the computational cost involved.

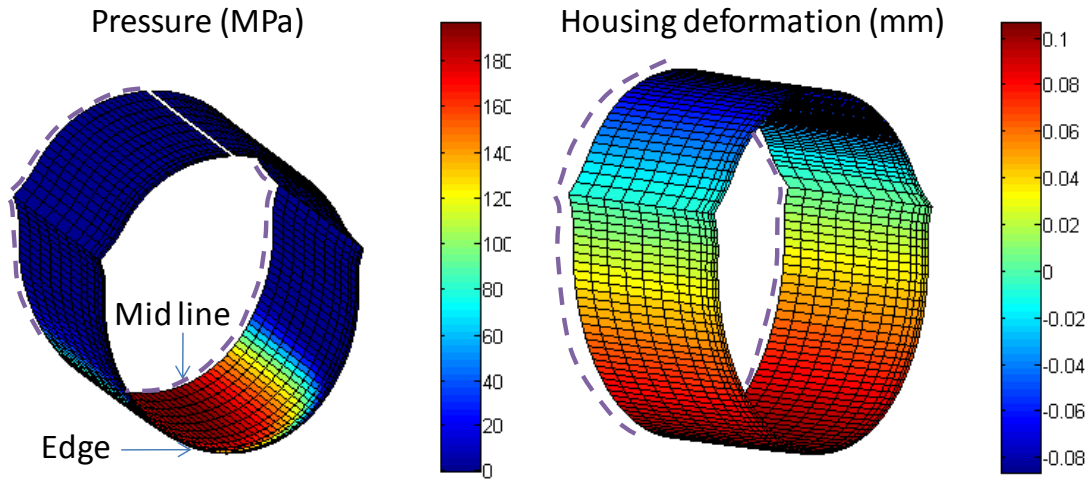

Figure 3. Film pressure and housing deformation at crank angle 180º of Sapphire rig test.

3. Results and discussion

3.1. Residual stresses

The forming analysis process took around 12 hrs on a 2.8 GHz processor with 2 GB of RAM memory. The solution showed that, at around 20% of the total travel of the punch, contact forces above 1000 N develop causing significant material yielding and deformation. The forming load increases as the bearing is driven to the bottom of the die due to the strain hardening material model and the contact area growth. The post-processing of results focused on the magnitude and distribution of the residual longitudinal stress, which becomes the tangential stress relative to the cylindrical frame of reference associated with the formed semi-circular shell bearing. As expected, the tangential stress was found to be discontinuous at the layers' interface showing high stress gradients across the layers' thickness; in contrast, it was almost constant across the component width. Its circumferential variations at the lining surface and the lining-backing interface at two key stages of the forming process are shown in Figure 4.

As indicated in Figure 4, the compressive tangential stress does not vary significantly through the thickness of the lining at end of the second stage of the simulation, that is, when the outer backing surface is in full contact with the die. As the bearing is separated from the die, elastic recovery occurs mainly driven by the reverse deformation of the backing layer, which provides most of the component stiffness. This generates tensile tangential stress in the lining; the tension at the surface is much greater than that developing at the lining-backing interface and considerably higher than the yield stress of the lining material (see Table 1); it also remains almost constant over a wide, centrally located portion of the component where the peak contact pressure occurs. As deformation progresses, an approximately constant compressive radial stress develops in that part of the bearing at a value around two times the

yield stress of the lining material. The shear stresses predicted by the simulation did not appear to be significant.

3.2. Stresses under service conditions

The analysis of the bearing based on accelerated Sapphire test data generated by SABRE-EHL was performed on the same computing facilities as those used for the forming simulation with a typical run providing the stresses over a complete journal cycle lasting about 24 hrs. The analyses performed showed that all stresses arising from the EHL regime varied substantially during the cycle depending on the film pressure profile and the associated housing deformation. The results for the total tangential stress along the surface of the bearing at an axial section 1.8 mm from the bearing edge are shown in Figure 5. Greater deformations and stresses were predicted in the central part of the lower bearing shell on the side of the connecting rod (see Figure 2). For this reason, the angular position ranges from 120° to 240° in Figure 5(a) where the spatial stress variation has been plotted for a range of crank angles within the third simulated cycle.

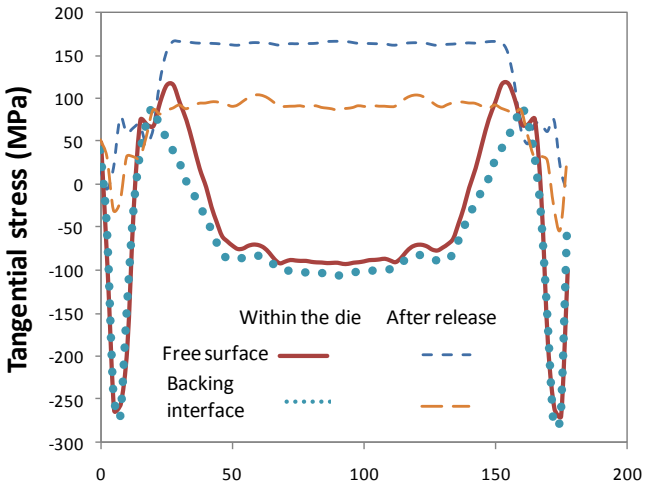

Figure 4. Circumferential variation of the tangential stress in the lining at the symmetry plane perpendicular to the axial direction.

For the assessment of fatigue performance, the same stress results were also plotted versus time represented by the crankshaft angular position; Figure 5(b) shows the stress cycles at four key circumferential locations. These plots reveal that there is essentially one representative crank cycle in the accelerated performance test and provide an indication of the range of mean stresses. Of equal importance is the distribution of the stress amplitudes, which were systematically evaluated over the whole lining surface and their contour map shown in Figure 6. It can be seen that they have been predicted to range from 60 to 220 MPa. However, it is worth noting by referring to Figure 5(b) that the highest amplitudes correspond to fully compressive stress cycles. This explains the high-cycle fatigue life of bearings, in spite of the extremely severe loading conditions.

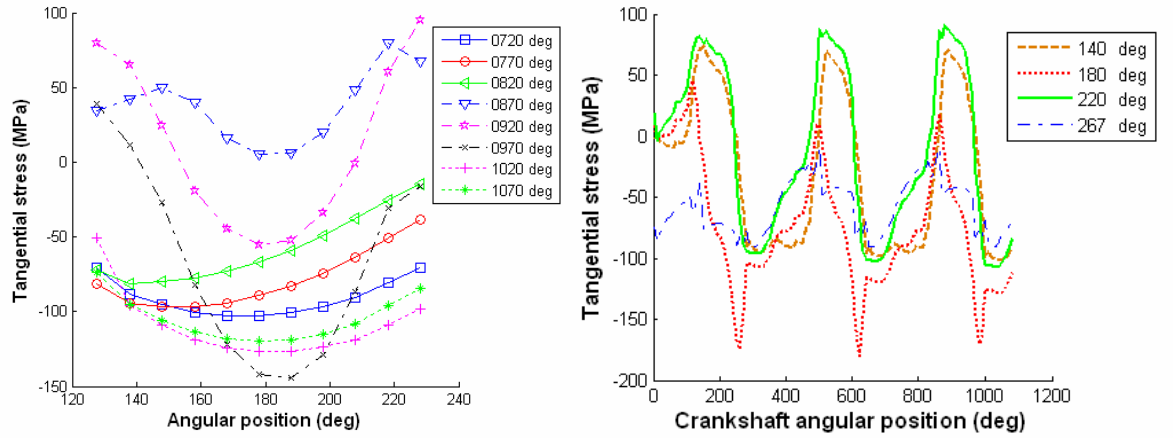

(a) (b)

Figure 5. Total tangential stress variation with (a) position and (b) time.

The stress amplitude contours in Figure 6 show that their maximum can be found around 190° in the circumferential direction and it has very small variation across the bearing width at that location. This is consistent with the position of the peak oil film pressure and the circumferential location of the damage observed during Sapphire rig tests. The latter appears closer to the edge rather than the middle of the bearing as anticipated from the numerical results, but still originates from the highest stress zone.

The high radial pressure applied to the bearing lining resulted in excessive plastic deformation and, in consequence, the appearance of high positive strains in the axial direction caused by the Poisson effect. This was also predicted by Bahai and Xu [3] and is clearly seen in the tangential plastic strain plots of Figure 7. The circumferential distributions of these strains shown in Figure 7(a) confirm that their high positive values, which correspond to the high pressure range of crank angle locations. The strain cycles shown in Figure 7(b) indicate considerable amplitude as well as positive mean value. The influence of such predictions on fatigue behaviour should be examined in conjunction with the stress cycles of Figure 5(b).

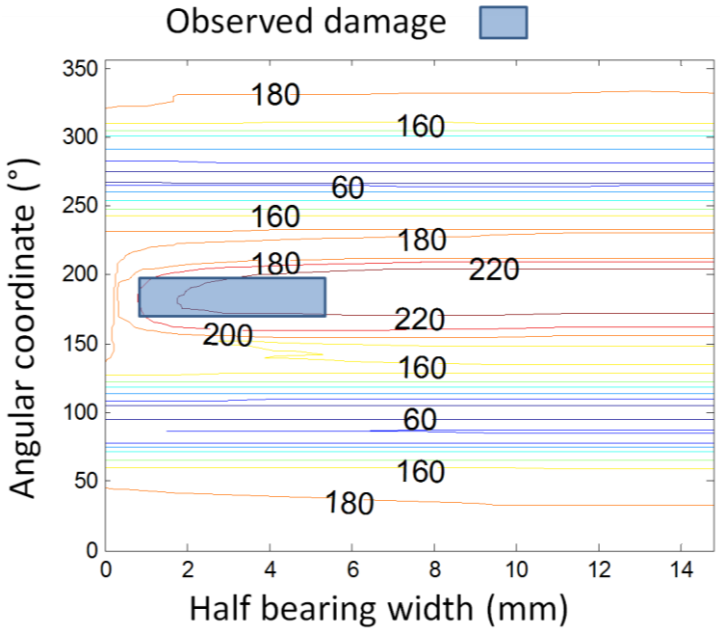

Figure 6. Stress amplitude contour map with observed damage in tests.

4. Concluding remarks

The stress analysis of a bearing under service conditions reveals that the inclusion of assembly and manufacturing conditions into the modelling leads to a better understanding of the significance of the stresses arising during the engine cycle to the bearing fatigue life. Stress estimates reveal that tensile tangential stresses exist along the lining surface despite the predominantly compressive state of stress caused by the assembly process and the oil film pressure. The latter is countered by the tensile residual stresses due to forming leading to a greater mean stress during the cyclic loading than originally thought.

As pointed out earlier, modern engines are designed to be considerably more compliant than the Sapphire rig. Under such more realistic conditions, the housing deformation is expected to play a more critical role in this problem with even greater tensile tangential stress values predicted especially when the inertial load is applied to the bearing shell opposite to the connecting rod thus causing greater deformation to the housing. There is therefore a need for further validation of the methodology and its application to bearings in real automotive engines.

The simulation of bearing response to the conditions generated during the accelerated performance test and its estimation of the stress and strain fields showed a good correlation between predictions of potential lining damage and experimental observations. The potential damage location was extended along the axial direction of the bearing showing similar stress amplitude values. The damage location along this direction could be largely influenced by the variability of the material microstructure and loading misalignments. Future work in this area will address the possible spread of damage while the

component remains in service by applying already developed crack growth methodology for layered material systems to bearings subjected to such conditions.

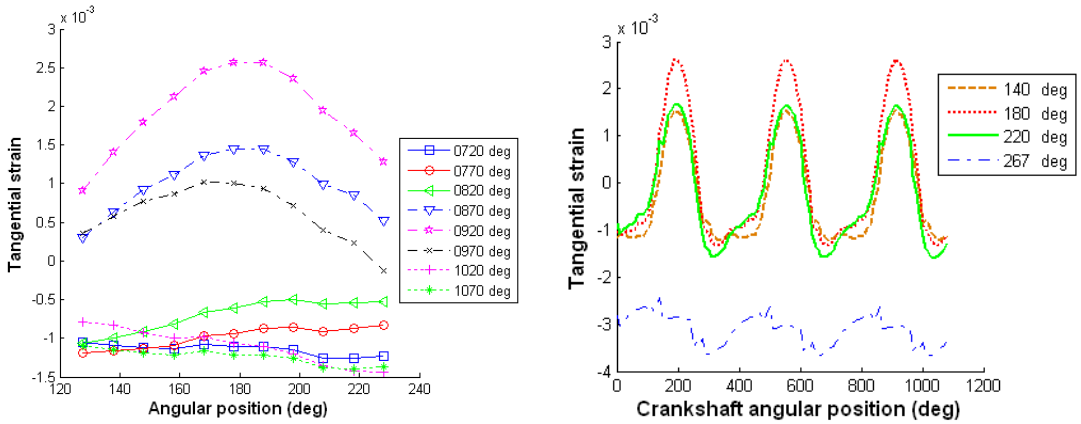

Figure 7. Tangential plastic strain variation with (a) position and (b) time.

References

[1] Martin FA, Garner DR, Adams DR. Hydrodynamic Aspects of Fatigue in Plain Bearings. J Lubr Technol-Trans ASME. 1981;103:150-156.

[2] McCallion H, Lotfi M. Tensile surface stresses and fatigue in plain journal bearings. Tribol Int. 1992;25(4):247-257.

[3] Bahai H, Xu H. Three-dimensional elastoplastic finite element and elastohydrodynamic analyses of journal bearings. Proc Inst Mech Eng Part C-J Eng Mech Eng Sci. 1997;211:143-152.

[4] Hacifazlioglu S, Karadeniz S. A parametric study of stress sources in journal bearings. Int J Mech Sci. 1996;38(8-9):1001-1015.

[5] Perez M, Thomazi C, Syngellakis S. Stress analysis of fluid-film bearings. In: Su D, editor. Proceedings of the International Conference on Gearing, Transmissions, and Mechanical Systems: Professional Engineering Publishing, 2000. p. 729-738.

[6] Xu H, Jones GJ, Aoyama S, Ushijima K, Okamoto Y, Kitahara K. Simulation of bearing wear and its Influence upon bearing performance based on elastohydrodynamic analysis. SAE 1999 World Congres. Detroit, Michigan; 1999.

[7] Mian AO, Merritt D, Wang D. The effect of crankshaft flexibility on the EHL of connecting rod bearings. SAE 2002 World Congres. Detroit, Michigan; 2002.

[8] ANSYS Release 11.0, ANSYS Academic Research. Canonsburg, PA 15317: ANSYS, Inc.; 2008.

[9] Avallone AE, Baumeister T, Sadegh A, editors. Marks' Standard Handbook for Mechanical Engineers: McGraw-Hill Professional; 2006.